



Single-step synthesis of dimethyl ether from syngas on Al₂O₃-modified CuO–ZnO–Al₂O₃/ferrierite catalysts: Effects of Al₂O₃ content

Yeong Jun Lee^a, Min Hye Jung^a, Jong-Bae Lee^b, Kwang-Eun Jeong^b, Hyun-Seog Roh^c, Young-Woong Suh^d, Jong Wook Bae^{a,*}

^a School of Chemical Engineering, Sungkyunkwan University (SKKU), Suwon, Kyeonggi-do 440-746, Republic of Korea

^b Korea Research Institute of Chemical Technology (KRICT), P.O. Box 107, Yuseong, Daejeon 305-600, Republic of Korea

^c Department of Environmental Engineering, Yonsei University, 1 Yonsei-dae-gil, Wonju, Gangwon 220-710, Republic of Korea

^d Department of Chemical Engineering, Hanyang University, Seoul 133-791, Republic of Korea

ARTICLE INFO

Article history:

Received 28 June 2013

Received in revised form 3 November 2013

Accepted 11 November 2013

Available online 17 December 2013

Keywords:

Single-step synthesis of DME

Bifunctional catalyst

CuO–ZnO–Al₂O₃

Al₂O₃-modified H-ferrierite zeolite

Syngas

Intrinsic activity

ABSTRACT

Single step synthesis of dimethyl ether (DME) from syngas on the bifunctional catalysts of CuO–ZnO–Al₂O₃ deposited on Al₂O₃-modified H-ferrierite was investigated to elucidate effects of Al₂O₃ modification of H-ferrierite in terms of CO conversion and DME yield. The enhanced catalytic activity was observed on the bifunctional catalysts at an optimum content of Al₂O₃ on H-ferrierite around 2.5–5 wt%. It is attributed to a higher dispersion of Al₂O₃ on H-ferrierite with an enhanced interaction of copper particles with Al₂O₃ modified H-ferrierite with a lower aggregation property by adjusting acidic sites and by increasing the dispersion of copper particles. The main role of Al₂O₃ on H-ferrierite is found to reduce strong acidic sites by depositing on the sites selectively, which resulted in showing a lower formation of byproducts. Both of copper surface area and amount of acidic sites are well correlated with an intrinsic activity (turn-over frequency; TOF), which revealed a structure-insensitive reaction character of a single-step synthesis of DME. The measurements of the dispersion of Al₂O₃ and copper particles with the number of acidic sites concomitantly were employed to verify the effects of Al₂O₃ modification of H-ferrierite though X-ray photoelectron spectroscopy, temperature-programmed methods and surface morphology characterizations.

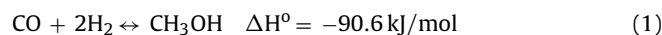
© 2013 Elsevier B.V. All rights reserved.

1. Introduction

Dimethyl ether (DME) synthesis through a single-step directly using syngas, which can be derived from a reforming reaction of hydrocarbons or gasification of biomass, has been largely investigated as an alternative renewable energy production. A biomass-derived CO₂-abundant syngas having a low H₂/CO ratio below one has been getting more attractive for the single-step synthesis of DME [1,2], since a bifunctional catalyst for a single-step synthesis of DME from biomass-derived syngas can be efficiently utilized even at low H₂/CO feed ratio due to its high activity for water–gas shift reaction. The utilization of DME as a renewable energy source has been also reported by replacing it with a liquefied petroleum gas, which has a high potential to minimize the emission of CO₂ and NO_x pollutants into the atmosphere by decreasing a global warming problem [3].

The general reactions for synthesizing DME involve two steps; the first step is for CO_x hydrogenation to methanol on CuO–ZnO based catalyst, and the subsequent second step is for dehydration of methanol to DME on solid-acid catalysts such as alumina or modified-zeolites [4–8]. The higher equilibrium conversion through a single-step reaction of DME synthesis from syngas on bifunctional catalyst can be obtained thermodynamically, since the second step of DME synthesis from methanol is much faster with a higher equilibrium conversion compared with the first step of methanol synthesis, which is characterized as a lower equilibrium conversion especially at a lower H₂/CO feed ratio. To overcome the thermodynamic conversion limitation, an application of bifunctional catalyst composed of Cu–ZnO and solid-acid component as well is beneficial for obtaining a higher conversion of reactants by producing surplus hydrogen through simultaneous water–gas shift (WGS) reaction during a single-step reaction as shown in following equations;

CO hydrogenation to methanol :



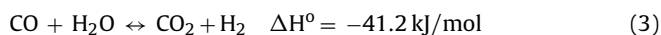
* Corresponding author. Tel.: +82 31 290 7347; fax: +82 31 290 7272.

E-mail address: finejw@skku.edu (J.W. Bae).

Dehydration to DME :



Water–gas shift reaction :



In general, solid acid catalysts such as alumina or zeolites reveal two sorts of acidic sites, which is known to be active sites for methanol dehydration to DME by shifts to higher conversions of CO_x and H_2 . However, the weak acidic sites act preferentially for methanol dehydration to DME, and the strong acidic sites are known to produce the byproducts such as light hydrocarbons by the possible decomposition of DME [9–12]. The strong acidic sites also interfere to form DME through the possible methanol to gasoline (MTG) process on strong acidic sites of zeolites. Therefore, it is necessary to remove strong acidic sites for the sake of obtaining a higher DME selectivity by adopting some modifiers on zeolites. From our previous works [10,11], Zr modifier on H-ferrierite zeolite was reported as one of the proper species for enhancing the DME selectivity by suppressing strong acid sites. In general, acidic sites of zeolites can be adjusted by employing alkali metals or rare earth metals such as K, Mg, Ca, and La, Ce, Fe and so on and by varying Si/Al ratios of zeolites [9,13–16,8]. In general, the catalytic activity for DME synthesis by methanol dehydration is much higher on zeolite-type catalysts compared with $\gamma\text{-Al}_2\text{O}_3$, due to the presence of a larger number of acidic sites on zeolites [13,14,17–20]. Therefore, Al_2O_3 component, which is also known to be active catalyst for dehydration of methanol on the weak acidic sites, can be also adopted to eliminate strong acidic sites on zeolites, by simultaneously controlling strong acidic sites and enhancing the number of acidic sites on Al_2O_3 -modified H-ferrierite zeolite. However, the researches for investigating the effects of Al_2O_3 modifier on zeolites for methanol dehydration are not much carried out based on our knowledge, especially for Al_2O_3 -modified H-ferrierite as solid–acid catalyst for single step synthesis of DME from syngas.

In the present investigation, we studied the effects of the Al_2O_3 modification of acid sites on H-ferrierite to compare with that of Zr-modified ferrierite in our previous works [10,11], which significantly altered the catalytic activity of methanol dehydration to DME. The different catalytic performances by varying a weight ratio of Al_2O_3 to H-ferrierite on bifunctional catalysts was explained by mainly characterizing the copper surface area and the number of acidic sites on $\text{CuO-ZnO-Al}_2\text{O}_3$ incorporated with Al_2O_3 -modified H-ferrierite for a single-step synthesis of DME.

2. Experimental

2.1. Catalyst preparation and activity test

The bifunctional catalysts were prepared by co-precipitation method using $\text{CuO-ZnO-Al}_2\text{O}_3$ component for CO hydrogenation on a solid–acid catalyst of Al_2O_3 -modified H-ferrierite zeolite. The Al_2O_3 -modified H-ferrierite was previously prepared by precipitation method using aluminum nitrate precursor ($\text{Al}(\text{NO}_3)_3 \cdot 6\text{H}_2\text{O}$) with $(\text{NH}_4)_2\text{CO}_3$ precipitant at a specific weight ratio of Al_2O_3 to H-ferrierite in an aqueous solution at 70°C , which possesses a $\text{SiO}_2/\text{Al}_2\text{O}_3$ molar ratio of around 20 supplied by Zeolyst with the surface area of around $366 \text{ m}^2/\text{g}$, and it was further confirmed by X-ray fluorescence analysis (supplementary Table S1). The specific weight ratio of Al_2O_3 to H-ferrierite varies from 0 to 10 wt%, and the solution was kept for aging for 2 h at the same temperature. After aging, the sample was dried for 24 h in an oven

kept at 110°C , followed by calcination at 500°C for 3 h under air environment.

Subsequently, the bifunctional catalysts were prepared by co-precipitation method in a slurry solution of Al_2O_3 -modified H-ferrierite kept at 70°C using the metal precursors of copper nitrate, zinc acetate, and alumina nitrate with $(\text{NH}_4)_2\text{CO}_3$ precipitant with an aging time of 2 h at 70°C . The sample was dried for 24 h in an oven at kept at 110°C . Finally, the bifunctional catalysts were calcined at 300°C for 3 h. The molar ratio of CuO , ZnO , and Al_2O_3 was fixed at 3.0:1.0:0.5, and the weight of CuO on Al_2O_3 -modified H-ferrierite was kept at a value of 1.75, to prepare $\text{CuO-ZnO-Al}_2\text{O}_3$ methanol synthesis catalyst combined with solid–acid component of Al_2O_3 -modified H-ferrierite. The as-prepared bifunctional catalysts are denoted as CZA/Al(x)-FER, where Al(x)-FER, C, Z, and A indicate Al_2O_3 -modified H-ferrierite, CuO , ZnO , and Al_2O_3 respectively, and x digit represents the weight ratio of Al_2O_3 to H-ferrierite such as 0, 2.5, 5, 10 wt%.

The catalytic activity was tested in a fixed bed tubular reactor with an outer diameter of 12.7 mm using catalyst of 0.4 g. Prior to reaction, the bifunctional CZA/Al-FER catalysts were reduced in a flow of 5 vol% H_2 balanced with N_2 at 300°C for 5 h to obtain an active metallic copper particles. Subsequently, syngas was fed to the reactor, which has a molar ratio of H_2/CO of 2.0 with an internal standard gas of N_2 . The reaction was carried out for around 20 h on stream at the following reaction conditions; $T=250^\circ\text{C}$, $P=3.5 \text{ MPa}$ and space velocity (SV)= $2000 \text{ ml/g}_{\text{cat}}/\text{h}$. The CO conversion and products distribution on the bifunctional catalysts were obtained from the steady-state average values for 5 h after 15 h on stream. The products were analyzed using an on-line gas chromatograph (Younglin GC, YL6100) using a thermal conductivity detector (TCD) to analyze N_2 , H_2 , CO and CO_2 and a flame-ionized detector (FID) to analyze methanol, DME, and other byproducts.

2.2. Characterization of the bifunctional catalysts

BET surface area of bifunctional CZA/Al-FER catalysts was measured by nitrogen adsorption method at -196°C by using a constant-volume adsorption apparatus (Micromeritics, ASAP-2020). The pore volumes were determined at a relative pressure (P/Po) of 0.99 and the pore size distribution of bifunctional catalysts was determined by BJH (Barett–Joyner–Halenda) model from the data of desorption branch of nitrogen isotherm.

The crystalline phases and particle sizes of copper species were characterized using powder X-ray diffraction (XRD) analysis using a Rigaku diffractometer with $\text{CuK}\alpha$ radiation in order to identify the metallic Cu, CuO , ZnO , $\gamma\text{-Al}_2\text{O}_3$, and ferrierite before and after reaction. The average particle size of copper species was calculated using the values of full width at half maximum (FWHM) of the most intensive XRD diffraction peaks at $2\theta=35.8^\circ$ for CuO on the fresh bifunctional catalyst, and $2\theta=43.3^\circ$ for metallic copper (Cu^0) on the used catalysts.

The surface area of metallic copper on the bifunctional catalysts was further measured by N_2O titration method. Prior to N_2O titration, the sample was reduced at 300°C for 5 h under a flow of 5 vol% H_2/N_2 , and the consumption of N_2O with a concomitant release of N_2 on metallic copper sites through the reaction, $\text{N}_2\text{O} + 2\text{Cu} = \text{Cu}_2\text{O} + \text{N}_2$, was analyzed by TCD equipped on BELCAT instrument. The surface area of metallic copper on the bifunctional catalysts before and after reaction for 20 h was calculated by assuming the concentration of $1.46 \times 10^{19} \text{ Cu atoms/m}^2$ with a molar ratio of 0.5 for $\text{N}_2\text{O}/\text{Cu}_s$ (Cu atom on surface) [17]. The elemental analysis of Ferrierite was analyzed using X-ray fluorescence (XRF; SEA5120).

To elucidate the reducibility of copper oxides on the bifunctional catalyst, temperature-programmed reduction (TPR) experiment was carried out. The sample was pretreated by flowing He up to 200°C for 1 h to remove the adsorbed water, and followed by

cooling to 50 °C. A 5 vol% H₂/He mixture was introduced in BEL-CAT instrument at a flow rate of 30 ml/min with a heating rate of 10 °C/min up to 600 °C. The effluent gas from reactor was passed through a molecular sieve to remove water formed during TPR experiment, and the amount of H₂ consumption was analyzed by TCD.

Temperature programmed desorption of ammonia (NH₃-TPD) was carried out using the H-ferrierite and fresh bifunctional catalyst to determine the number of acidic sites and its acidic strength. Around 0.1 g of sample was initially flushed with a He flow at 250 °C for 2 h, and subsequently cooled down to 100 °C and then the sample was saturated with NH₃. After NH₃ exposure, the sample was purged under a He flow until it reached an equilibrium point, then it was allowed TPD experiment using the BELCAT instrument in the temperature range of 100–600 °C with a heating rate of 10 °C/min and kept at that temperature for 10 min.

The Fourier-transformed infrared-spectroscopy (FT-IR) was adopted to characterize the structures of metal oxides on the fresh and used catalysts. The bifunctional CZA/Al-FER catalysts are composed of several kinds of bonds of metal oxides such as CuO, ZnO and Al₂O₃ and so on. By observing the different intensities of metal oxide bonds, the dispersion of CuO between copper and/or aluminum and oxygen bonds assigned the characteristic peaks of 697 and 1730 cm⁻¹ was compared on the bifunctional catalysts [21,22].

The electronic states of surface copper species were characterized by using X-ray photoelectron spectroscopy (XPS; (ESCALAB MK-II)) analysis. During the experiment, Al-K α monochromatized line (1486.6 eV) was adopted and the vacuum level was kept around 10⁻⁷ Pa. The fresh CZA/Al-FER was previously pressed to a thin pellet and the binding energy (BE) was corrected with the reference BE of C1s (284.6 eV).

The particle sizes of copper oxides and the variation of surface morphologies after reaction for 20 h were further characterized by using the transmission electron microscopy (TEM; TECNAI G2 instrument) to support the results of XRD analyses and N₂O titration.

3. Results and discussion

The physicochemical properties of copper surface area and the number of acidic sites can largely alter the catalytic performances by changing the reaction rates of CO hydrogenation and dehydration of methanol to DME simultaneously. The roles of acidic sites on solid-acid zeolite are more dominant factors for varying the total reaction rates on the bifunctional CZA/Zr-FER catalysts as reported in our previous works [10,11]. Therefore, Al₂O₃-modified H-ferrierite can also act as a proper dehydration catalyst by suppressing the strong acidic sites, and it can also affect the dispersion of CuO–ZnO–Al₂O₃ particles by changing the surface properties of H-ferrierite. The correlation of copper surface area and the number of acidic sites with catalyst performances was further investigated on the CZA/Al-FER catalysts based on our previous works [10,11].

3.1. Physicochemical properties of the CZA/Al-FER catalysts

The surface area, pore volume, and average pore diameter of CZA/Al-FER catalysts were significantly altered by the amount of Al₂O₃ modification of H-ferrierite, and the results are summarized in Table 1 and Fig. 1. For comparison, the surface area and pore size distribution of H-Ferrierite are summarized in Supplementary Fig. S1, and its surface area was found to be 366.2 m²/g. The surface area is found to be in the range of 120.7–175.1 m²/g, and it is maximized on CZA/Al(2.5)-FER catalyst with the value of 175.1 m²/g. However, the surface area gradually decreased to 120.7 m²/g by increasing Al₂O₃ content on H-ferrierite. The pore volume of CZA/Al-FER

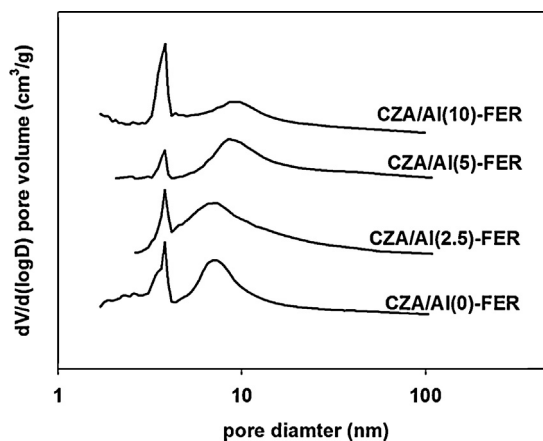


Fig. 1. Pore size distribution of the fresh CZA/Al-FER catalysts.

catalysts is found to be in the range of 0.27–0.34 cm³/g, and the trend is in line with the surface area variation. The average pore diameter was found to be above 6.7 nm, and the pore size was increased by increasing Al₂O₃ content, and it showed a maximum value of 10.0 nm on CZA/Al(5)-FER catalyst. The pore size distribution on the CZA/Al-FER catalysts was also shown in Fig. 1, and the bimodal pore size distribution with the distinctive peaks at around 4 and 10 nm in diameter was observed on all CZA/Al-FER catalysts. The first narrow small pore can be possibly attributed to the intracrystalline pores of CuO–ZnO–Al₂O₃ particles and Al₂O₃-modified H-ferrierite powders itself, and the second broad large pores could be ascribed to the inter-crystalline pores between CuO–ZnO–Al₂O₃ particles and Al₂O₃-modified H-ferrierite, which was previously observed on CuO–ZnO–Al₂O₃-based catalysts [11,23]. With the increase of Al₂O₃ content on H-ferrierite, the large pores at around 10 nm shifted to larger pore diameters by increasing the intensities, except for CZA/Al(10)-FER catalyst. This observation suggests the abundant formation of inter-crystalline pores of CuO–ZnO–Al₂O₃ particles on Al₂O₃-modified H-ferrierite by changing the surface properties of H-ferrierite, and it was contributed to the increase of average pore size on CZA/Al(5)-FER catalyst as shown in Table 1. The co-presence of bimodal-size pores is reported to enhance catalytic performances by increasing the transport rates of reactants and products to outer surfaces of inter-crystalline pores [11,19].

The XRD patterns of CZA/Al-FER catalysts before reaction were displayed in Fig. 2. The characteristic multiple diffraction peaks of

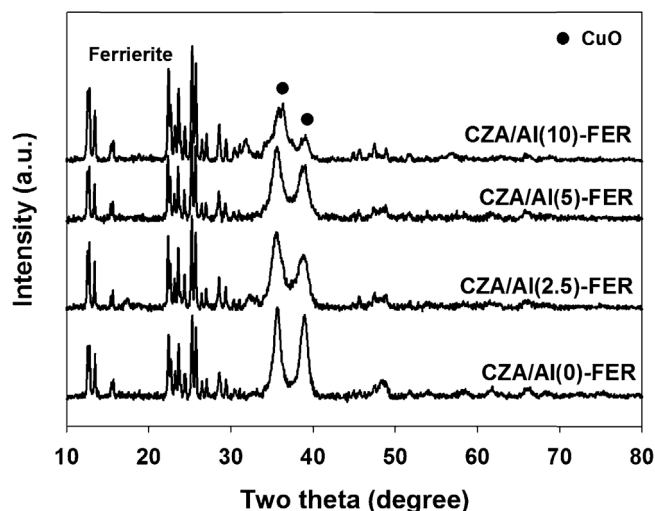


Fig. 2. XRD patterns of the CZA/Al-FER catalysts before reaction.

Table 1
Physicochemical properties of the bifunctional CZA/Al-FER catalysts.

| Notation ^a | BET surface area (m ² /g) | Pore volume (cm ³ /g) | Average pore diameter (nm) |
|-----------------------|--------------------------------------|----------------------------------|----------------------------|
| CZA/Al(0)-FER | 160.0 | 0.27 | 6.7 |
| CZA/Al(2.5)-FER | 175.1 | 0.34 | 7.8 |
| CZA/Al(5)-FER | 155.4 | 0.30 | 10.0 |
| CZA/Al(10)-FER | 120.7 | 0.29 | 7.3 |

^a The bifunctional CZA/Al-FER catalysts are denoted as CZA/Al(x)-FER, where Al(x)-FER, C, Z, and A indicates Al₂O₃-modified H-ferrierite, CuO, ZnO, and Al₂O₃, respectively. The x digit represents the weight ratio of Al₂O₃ to H-ferrierite zeolite.

Table 2
Acidity, particle sizes and metallic copper surface areas on the bifunctional CZA/Al-FER catalysts.

| Notation | Acidic sites (mmolNH ₃ /g) from NH ₃ -TPD | | | Particle size of CuO and Cu ⁰ (nm) from XRD analysis | | Cu surface area (m ² /g _{Cu}) from N ₂ O titration | | I ₂ /I ₁ ratio from XPS analysis ^a | [Cu surface area (after)] × [acidic site (total)] |
|-----------------|---|--------------------------|-------|---|-------------------------|--|------|---|---|
| | T ₁ (<400 °C) | T ₂ (<600 °C) | Total | CuO (before) | Cu ⁰ (after) | Fresh | Used | | |
| CZA/Al(0)-FER | 10.6 | 3.2 | 13.8 | 7.8 | 16.8 | 3.8 | 5.40 | 1.19 | 57.0 |
| CZA/Al(2.5)-FER | 13.1 | 3.6 | 16.7 | 4.9 | 7.2 | 10.1 | 6.95 | 1.58 | 90.7 |
| CZA/Al(5)-FER | 12.2 | 4.1 | 16.3 | 5.2 | 10.3 | 8.1 | 7.02 | 1.80 | 85.6 |
| CZA/Al(10)-FER | 11.7 | 2.7 | 14.4 | 7.2 | 24.1 | 3.1 | 4.27 | 1.36 | 50.1 |

^a The ratio (I₂/I₁) is defined as the intensity of Cu⁺ at 930 eV (assigned to I₁) to shoulder peak at around 932 eV (assigned to I₂).

H-ferrierite were observed below $2\theta = 30^\circ$, and the larger diffraction peak intensity of CuO particles were observed at $2\theta = 35.8$ and 38.0° . All CZA/Al-FER catalysts showed the characteristic H-ferrierite structures even after coprecipitation of CuO–ZnO–Al₂O₃ components on AlO₃-modified H-ferrierite without a significant variation of diffraction peak intensities. The particle sizes of CuO on the fresh catalysts were summarized in Table 2. It was calculated from the values of FWHM using Scherrer equation at $2\theta = 35.6^\circ$ for CuO species. The particle size of CuO was found to be in the range of 4.9–7.8 nm, and it was decreased by modifying H-ferrierite with Al₂O₃ compared with unmodified CZA/Al(0)-FER catalyst. The average particle size of CuO was minimized on CZA/Al(2.5)-FER catalyst with a value of 4.86 nm, and it can be attributed to the variation of surface acidity induced from Al₂O₃ modification of H-ferrierite by changing CuO-support interaction. The larger amount of Al₂O₃ distribution on H-ferrierite surfaces can be the reason for the enhanced dispersion of CuO–ZnO–Al₂O₃ with a formation of smaller CuO particles, especially on CZA/Al(2.5)-FER, which was explained by the following results of acidity measurement and N₂O titration.

3.2. Surface properties of CZA/Al-FER catalysts (FT-IR, TPR, XPS, and NH₃-TPD)

To verify the types of metal oxides and the degree of formation on CZA/Al-FER catalysts, FT-IR experiments were carried out using the fresh and used bifunctional catalysts and they are shown in Fig. 3. The characteristic peaks of CuO bonds were confirmed by FT-IR at the wavenumbers of around 697 and 1730 cm⁻¹, and other peaks assigned to the wavenumbers of 1090, 1207 and 3300 cm⁻¹ can be assigned to SiO, AlO and OH stretching, respectively [24,25]. The highly-dispersed copper oxides on CZA/Al(5)-FER catalyst were supported by observing the intense vibration band at 697 and 1730 cm⁻¹ which can be assigned to characteristic CuO absorption band on CZA/Al(5)-FER catalyst. The FT-IR peaks observed on CZA and Al(5)-FER samples also support the proper assignment of characteristic peaks of metal oxides as shown in Fig. 3(A). In addition, the decreased intensity of shoulder peak at 1207 cm⁻¹ and increased intensity at 1090 cm⁻¹ on the CZA/Al(5)-FER can also be attributed to the deteriorated silica framework, which is possibly attributed to strong interaction of CuO due to the well dispersion of CuO on Al₂O₃-modified H-ferrierite [11]. The optimum calcination temperature of 300 °C for CZA/Al-FER catalyst was also confirmed by observing the higher intensity of these

characteristic peaks as shown in Supplementary Fig. S2. Furthermore, the larger peak intensity at 1090 cm⁻¹ can also support the increase of Cu–O–Si population on the H-ferrierite surface due to the phase segregation of Al–O–Si linkages [26]. The high dispersion of CuO species interacting with H-ferrierite was obtained on

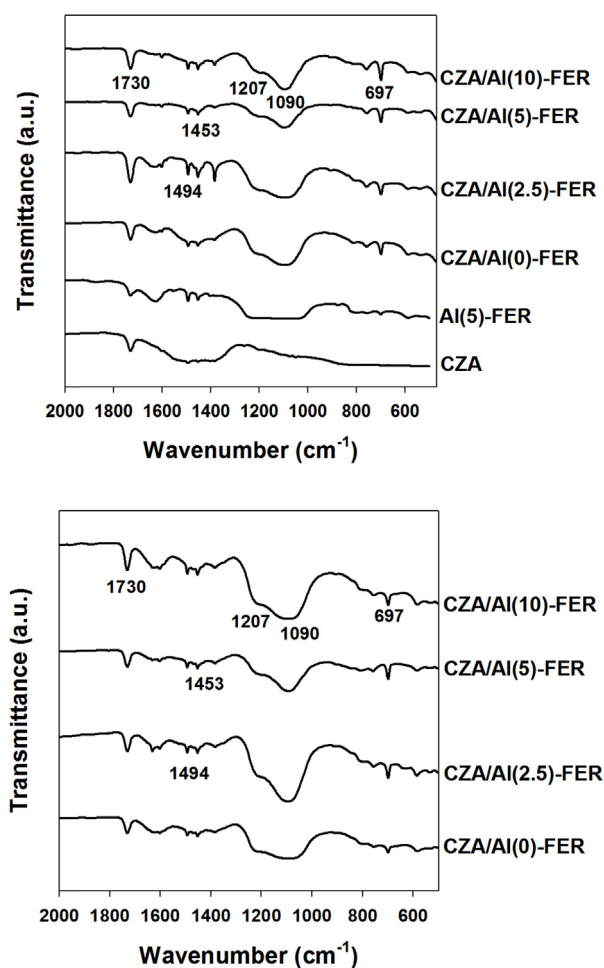


Fig. 3. Spectra of Fourier-transformed infrared spectroscopy of CZA/Al-FER catalysts before (A) and after reaction (B).

CZA/Al(5)-FER catalyst calcined at 300 °C. As shown in Fig. 3(A) for CZA/Al-FER before reaction, which were calcined at 300 °C with a different amount of Al₂O₃ modification, the characteristic peaks of CuO at the wavenumbers of 697 and 1730 cm⁻¹ were maximized on CZA/Al(2.5)-FER and CZA/Al(5)-FER catalyst, which suggests a higher dispersion of CuO on Al₂O₃-modified H-ferrierite. In addition, the high peak intensities at 1090 and 1207 cm⁻¹ revealed the strong interactions of CuO with Al₂O₃-modified H-ferrierite. These characteristic peaks were also verified by characterizing the Al₂O₃-modified H-ferrierite and Cu–ZnO–Al₂O₃ and by observing higher intensity at 1730 cm⁻¹ for Cu–ZnO–Al₂O₃ components and higher intensity in the ranges of 1250–1700 cm⁻¹ on Al₂O₃-modified H-ferrierite as shown in Fig. 3(A). In general, the higher dispersion of Cu–ZnO–Al₂O₃ species on H-ferrierite is responsible for the higher CO conversion and DME selectivity as reported from our previous researches [10,11,19,20,23,27]. Interestingly, these characteristic peaks with high intensities as shown in Fig. 3(B) retained even after reaction of 20 h, and the superior characters on CZA/Al(2.5)-FER and CZA/Al(5)-FER catalyst can be explained by comparing with the variation of copper surface area according to the types of bifunctional catalysts. From the results of FT-IR analysis, the optimum concentration of Al₂O₃ modifier on H-ferrierite by forming a proper interaction with CuO is important to obtain a higher dispersion of CuO particles on Al₂O₃-modified H-ferrierite. Even though FT-IR peaks are not significantly altered by modifying with a different amount of Al₂O₃ on H-ferrierite, the small variation of characteristic peak intensities of CuO before and after reaction on CZA/Al(2.5)-FER and CZA/Al(5)-FER catalyst suggest the high stability of those catalysts by suppressing the significant aggregation of Cu–ZnO–Al₂O₃ particles. The suppressed aggregation of CuO on the properly Al₂O₃-modified H-ferrierite is also beneficial for decreasing the amount of strong acidic sites and reducibility of CuO species simultaneously. The strong interactions of CuO with Al₂O₃-modified H-ferrierite were confirmed by characterizing CZA/Al-FER catalysts using XPS analysis as shown in Supplementary Fig. S3. The BE of Cu2p_{3/2} photoelectron spectra of the fresh CZA/Al-FER catalysts can be assigned to 930 eV for Cu⁺ and 932 eV for Cu²⁺ with the characteristic satellite peaks around 940 eV. As shown in Table 2, the intensity ratio of Cu⁺ at 930 eV (assigned to I₁) to shoulder peak of Cu²⁺ at around 932 eV (assigned to I₂) is found to be in the range of 1.19–1.80, and the ratio is maximized on CZA/Al(5)-FER catalyst with the value of 1.80. The more detailed results are summarized in Supplementary Table S2. The increased shoulder peak assigned to Cu²⁺ species on CZA/Al(2.5)-FER and CZA/Al(5)-FER catalysts suggest the strong interaction of CuO with Al₂O₃-modified H-ferrierite, and it also reveals a small variation of copper particle size with a well-dispersed two-dimensional Cu⁰–Cu⁺ layer even after reaction [28].

The reducibility of CZA/Al-FER catalysts was characterized by TPR experiment, and the maximum reduction temperatures were observed below 300 °C as shown in Fig. 4. The reduction behaviors of CuO on the CZA/Al-FER catalysts largely altered the catalytic activity and stability by changing the surface area of metallic copper and by influencing the extent of aggregation of active metals. In general, the fast reaction rate of this consecutive reaction was attributed to the higher formation rate of methanol from syngas on metallic copper surfaces due to the lowest activation barrier for the adsorption pathway of two contiguous methanol molecules to generate DME molecule [10,11,29]. Since the methanol formation from syngas, which is a first step for DME production via dehydration of methanol, occurs on the metallic copper surfaces, the higher surface area of copper on Al₂O₃-modified H-ferrierite is an important factor for a fast consecutive reaction to DME from syngas [10]. The reducibility of copper oxides on CZA/Al-FER was verified by TPR experiments, and high reduction degree on all bifunctional catalysts below 300 °C was observed as shown

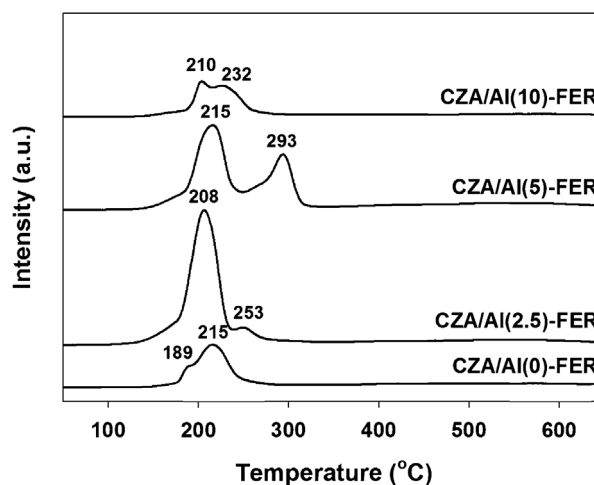


Fig. 4. TPR profiles of the fresh CZA/Al-FER catalysts.

in Fig. 4. The reduction peak around 210 °C can be attributed to CuO reduction on Cu–ZnO–Al₂O₃ component, and the shoulder peaks at a higher temperature of above 250 °C can be assigned to the strongly interacted CuO species with Al₂O₃-modified H-ferrierite. The observed high intensity at a higher temperature at 293 °C on CZA/Al(5)-FER catalyst suggests the heterogeneously distributed CuO particles with a strong metal-support interaction on Al₂O₃-modified H-ferrierite as confirmed by XPS and FT-IR analyses. In general, the formation of homogeneous microstructures of CuO–ZnO at similar chemical composition is important to obtain a higher CO conversion due to the easy formation of a smaller copper particles with a higher surface area [30], which can be confirmed by observing Gaussian pattern of reduction peak as assigned in low temperature peaks around 210 °C on all CZA/Al-FER catalysts. However, in terms of catalyst stability, the presence of shoulder peak at a higher temperature can be assigned to the strongly interacted CuO with Al₂O₃-modified H-ferrierite, which is responsible for the lower aggregation of copper particles during a single-step DME synthesis reaction. Interestingly, the shoulder peak at a higher temperature was observed on CZA/Al(5)-FER catalyst with the highest intensity, and the peak was observed on all CZA/Al-FER catalysts except for CZA/Al(0)-FER catalyst. The peak split of reduction peaks was observed on CZA/Al(10)-FER catalyst, and it also suggests the heterogeneous distribution of CuO on Al₂O₃-modified H-ferrierite due to the uneven distribution of Al₂O₃ on H-ferrierite surfaces at a higher Al₂O₃ concentration. TPR profiles on CZA/Al(2.5)-FER and CZA/Al(5)-FER catalyst suggest that CuO particles are well distributed on Al₂O₃-modified H-ferrierite surfaces by forming CuO–ZnO matrix. The homogeneous distribution by forming small particles of CuO and strong interaction with Al₂O₃-modified H-ferrierite on CZA/Al(5)-FER catalyst can largely reduce the aggregation of copper particles during the reaction. The degree of reduction of CuO–ZnO–Al₂O₃ can be also strongly affected by the dispersion of Al₂O₃ on H-ferrierite, which is further verified by NH₃-TPD and the copper surface area measurement through N₂O titration method.

The different reduction patterns of CZA/Al-FER catalysts can be also affected by the amount of surface acidic sites, therefore, their characteristics were analyzed by NH₃-TPD experiments as shown in Fig. 5 and the results were summarized in Table 2. The different distribution of Al₂O₃ modifier on H-ferrierite eventually alters the acidic properties of the CZA/Al-FER catalysts by changing the degree of surface blockage of acid sites through the deposition of CuO–ZnO–Al₂O₃ components [31]. The characteristic NH₃-TPD peaks and their amount of acidic sites of H-Ferrierite itself are summarized in Supplementary Fig. S4. The weak and strong

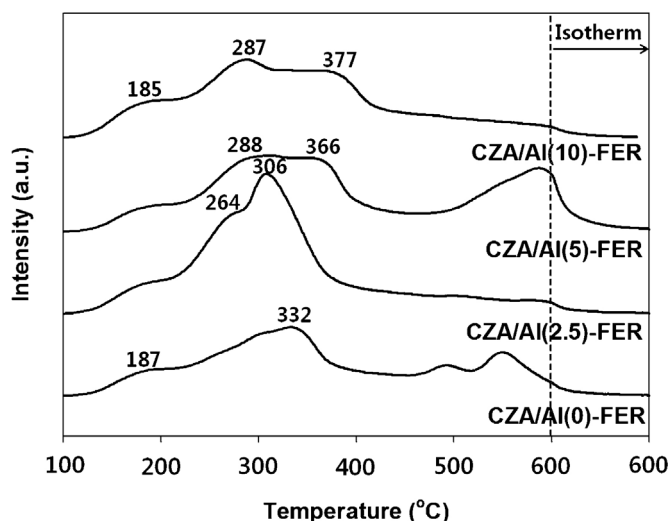


Fig. 5. NH_3 -TPD profiles of the fresh CZA/Al-FER catalysts.

acidic sites are found to be 37.4 and 15.9 mmolNH_3/g , respectively, and the amounts of acidic sites were significantly reduced after CZA/Al-FER catalyst preparation, especially for the strong acidic sites. Therefore, the extent of surface modification of acidic sites can be estimated by comparing the particle size of CuO and the amount of acidic sites on the CZA/Al-FER catalysts simultaneously. As shown in Fig. 5, two distinguishable desorption peaks can be divided with the peaks appearing below 400 °C (T_1) and 400–600 °C (T_2), assigned to weak and strong acidic sites, respectively [19,20,27]. The desorption peak appearing below 400 °C is attributed to the weakly adsorbed NH_3 , and the peak above 400 °C is for the strongly adsorbed NH_3 molecules or desorption of H_2O from main frameworks of CuO–ZnO– Al_2O_3 or Al_2O_3 -modified H-ferrierite. The weak acidic sites (peak I) plays an important role for methanol dehydration to DME, and the formation of byproducts such as hydrocarbons and CO_2 can be enhanced with the increase of strong acidic sites (peak II) by the possible reforming reaction of DME and methanol [3,9–11]. The activity of single step DME synthesis from syngas significantly depends on the amount of acidic sites on Al_2O_3 -modified H-ferrierite and that of metallic copper sites. The summarized quantities of acidic sites on CZA/Al-FER catalysts are shown in Table 2. By varying the amount of Al_2O_3 modifier on H-ferrierite, the weak acidic sites (peak I) were maximized on CZA/Al(2.5)-FER catalyst with the value of 12.2 mmolNH_3/g , and its values was found to be smallest on the unmodified CZA/Al(0)-FER catalyst with the value of 10.6 mmolNH_3/g . The different acidic sites can be correlated with the dispersion of Al_2O_3 species on H-ferrierite, and the highest dispersion of Al_2O_3 was observed on CZA/Al-FER catalysts with Al_2O_3 concentration of 2.5–5.0 wt%. The variation of strong acidic sites (peak II) and total acidic sites showed the almost same trend like weak acidic sites, with the values of 13.8–16.7 mmolNH_3/g . The amount of Al_2O_3 on H-ferrierite can be essential for enhancing catalytic performances by maximizing the weak acidic sites, and it also alters Cu–ZnO– Al_2O_3 dispersion by forming a small particles of copper of 4.9 and 5.2 nm in size on the fresh CZA/Al(2.5)-FER and CZA/Al(5)-FER catalyst as confirmed by XRD analysis (Fig. 2 and Table 2). The formation of small copper particles on the fresh catalysts was also verified by measuring the surface area of metallic copper through N_2O titration as shown in Table 2. The surface area of copper was found to be in the range of 3.1–10.1 m^2/g , and its area was maximized on the fresh CZA/Al(2.5)-FER catalyst with the value of 10.1 m^2/g (copper) which is in line with the results of XRD analysis. The lower value of copper surface area on CZA/Al(10)-FER catalyst is attributed to the

small amount of acidic sites on Al_2O_3 -modified H-ferrierite with uneven distribution of Cu–ZnO– Al_2O_3 particles since there is not sufficient sites to interact with the precipitates of Cu–ZnO– Al_2O_3 particles [19,20,23,27]. Interestingly, the amount of weak and total acidic sites on CZA/Al-FER catalysts showed a volcano curve, and the this observation can explain that the effects of Al_2O_3 modification of H-ferrierite is related with the enhancing the weak acidic sites by adding Al_2O_3 component and small copper particle formation, which is beneficial for obtaining higher catalytic performance of single-step DME synthesis.

3.3. Catalytic activity correlated with acidic sites and surface area of metallic copper

The CZA/Al-FER catalysts were further characterized using the used catalysts after 20 h to elucidate the effects of Al_2O_3 modification of H-ferrierite after the stabilization of catalytic activity using XRD, FT-IR, N_2O titration, and TEM analyses. The particle size of copper was significantly altered after reaction, especially on CZA/Al(0)-FER and CZA/Al(10)-FER catalyst, which showed a lower dispersion (large particle size of CuO) of Cu–ZnO– Al_2O_3 particles on H-ferrierite surfaces. From XRD analysis on the used CZA/Al-FER catalysts as shown in Table 2 and Supplementary Fig. S5, the characteristic metallic copper peak at $2\theta = 43.3^\circ$ were observed on all CZA/Al-FER catalysts without a significant variation of XRD intensities of characteristic peaks of H-ferrierite, which suggests that no significant changes of the Al_2O_3 -modified H-ferrierite structures. The peak intensity of metallic copper was found to be larger on CZA/Al(10)-FER catalyst, and smallest on CZA/Al(2.5)-FER catalyst. The calculated particle size of metallic copper after reaction, summarized in Table 2, is found to be in the range of 7.2–24.1 nm. The smallest particle size of metallic copper of 7.2 nm without a mild aggregation of copper particles was observed on CZA/Al(2.5)-FER catalyst, which showed a higher dispersion of Cu–ZnO– Al_2O_3 species on H-ferrierite and largest amount of acidic sites from NH_3 -TPD. The significant aggregation of copper particles with a size of 24.1 nm was observed on CZA/Al(10)-FER catalyst which showed a lower amount of acidic sites. This was also supported by the results of FT-IR analyses on used catalysts as shown in Fig. 3(B). The larger characteristic peaks of Cu–O stretching bond at the wavenumbers of 710 and 1730 cm^{-1} were observed on CZA/Al(2.5)-FER catalyst, which supports the high dispersion of CuO on Al_2O_3 -modified H-ferrierite even after reaction. The larger peak intensities at 1207 and 1090 cm^{-1} were also observed on CZA/Al(2.5)-FER and CZA/Al(5)-FER which possessed a stronger interaction of CuO with Al_2O_3 -modified H-ferrierite (results of FT-IR and XPS analysis). To further support the particle size variation after reaction for 20 h, copper surface area measurements were carried on the used CZA/Al-FER catalysts as summarized in Table 2. The surface areas were significantly decreased, and the values were found to be in the range of 4.3–6.95 m^2/g . The smallest variation of surface area of metallic copper were found on CZA/Al(2.5)-FER and CZA/Al(5)-FER catalyst with the values of 6.95 and 7.02 m^2/g , which were characterized as a smaller particle formation of CuO and larger amount of acidic sites. Therefore, the amount of acidic sites after Al_2O_3 modification of H-ferrierite can alters the particle size of CuO as well as catalytic stability by suppressing aggregation of copper species during the reaction.

In addition, the morphologies and size distribution of copper particles on CZA/Al(0)-FER and CZA/Al(5)-FER catalyst before and after reaction were characterized by TEM analyses as shown in Fig. 6. The sphere type particles in the size of 5–10 nm were homogeneously distributed on the fresh CZA/Al-FER catalysts, and the size of CuO is found to be smaller on CZA/Al(5)-FER which is in line with the results of XRD and N_2O titration. However, a significant aggregation of copper particles was observed on both

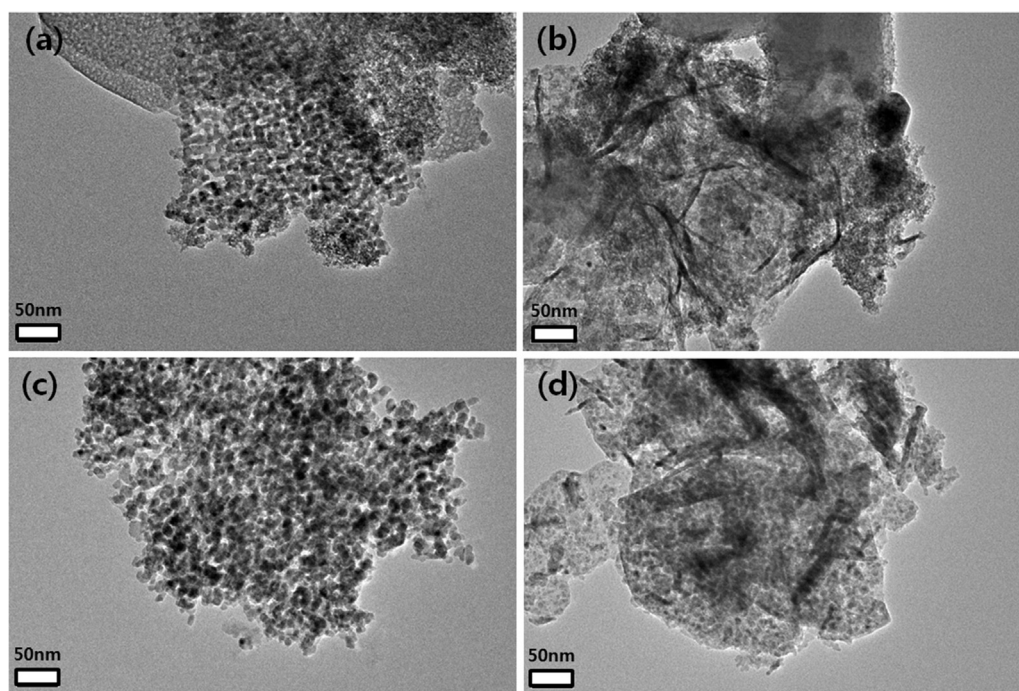


Fig. 6. TEM images of CZA/Al-FER catalysts before and after reaction. (a) After reaction of CZA/Al(0)-FER, (b) before reaction of CZA/Al(0)-FER, (c) before reaction of CZA/Al(5)-FER, (d) after reaction of CZA/Al(5)-FER

catalysts after reaction by forming larger particles up to 50 nm in size, and its shapes are mainly a rod-type aggregate on both catalysts. The aggregation is less significant on CZA/Al(5)-FER catalyst which is also in line with the results of XRD and N_2O titration. Especially, the small copper particles of 10 nm in size are more abundant on CZA/Al(5)-FER catalyst compared with that of CZA/Al(0)-FER catalyst. This can be attributed to the strong interaction of Cu–ZnO– Al_2O_3 particles on the Al_2O_3 -modified H-ferrierite surfaces as confirmed by TPR experiment by showing a larger shoulder peak at higher reduction temperature region, and by NH_3 -TPD with a larger number of acidic sites which can be supported by the observation of FT-IR.

The catalytic performance at steady state after 15 h on stream was summarized in Table 3. The CO conversion and DME selectivity were found to be higher on CZA/Al(2.5)-FER and CZA/Al(5)-FER catalyst compared with the unmodified CZA/Al(0)-FER catalyst. Higher CO conversions of 61.8–62.1% and higher DME selectivity of 93.4–91.5% were observed on those catalysts, and the lower CO conversion of 46.6% and DME selectivity of 87.4% were observed on CZA/Al(0)-FER catalyst. CO_2 formation showed a same trend with CO conversion, i.e., a higher CO conversion is responsible for a higher CO_2 formation rate due to the enhanced WGS reaction. Interestingly, the selectivity of byproducts such as light hydrocarbons was higher on CZA/Al(0)-FER catalyst, which possessing a relatively larger strong acidic sites by possibly enhancing the transformation of DME/methanol to hydrocarbons [3,9–11] compared with the other catalysts. In addition, reaction rate defined as the reacted CO mol/ g_{cat}/h , and turn over frequency (TOF) defined as the number of reacted CO molecules/surface metallic copper atom/second, were also calculated using the values of copper surface area after reaction and the results are summarized in Table 3. The reaction rates were found to be in the range of 0.026–0.037 mol/ g_{cat}/h and it is maximized on CZA/Al(5)-FER catalyst. The variation of reaction rates are similar with the CO conversions, but TOF values are almost similar on all CZA/Al-FER catalysts with the values of 0.059–0.069 molecules/Cu atom/s by monotonously increasing with the increase of Al_2O_3 content on H-ferrierite. This observation suggests the characteristics of structural insensitive reaction of

single step synthesis reaction of DME from syngas as reported in our previous work [10]. The Al_2O_3 -modified H-ferrierite on CZA/Al-FER catalysts showed an enhanced catalytic performance since the strong acidic sites on H-ferrierite were properly modified by introducing Al_2O_3 , and Al_2O_3 modifier also suppressed the significant aggregation of copper particles by enhancing the interaction of copper particles with Al_2O_3 -modified H-ferrierite. The results were supported by the FT-IR, XPS, NH_3 -TPD, XRD, TEM, and N_2O titration. Even though CO_2 formation rate is proportional to CO conversion due to the enhanced WGS reaction with the increase of CO conversion, the byproduct formation like light hydrocarbons are significantly suppressed by introducing Al_2O_3 modifier on H-ferrierite, which is attributed to the reduced reforming reaction of DME/methanol on the strong acidic sites [11,18,19]. Therefore, CO conversion and DME yield on CZA/Al-FER catalysts are strongly related with two factors such as the surface area of metallic copper for CO hydrogenation to methanol and the amount of acidic sites for dehydration of methanol to DME in a single-step reaction.

Finally, we modified our previous results by combining the present results [10] to correlate the reaction rate and intrinsic activity (TOF) of CZA/Al-FER catalysts with respect to the product values of the amount of acidic sites ($mmolNH_3/g_{cat}$) and surface area of metallic copper (m^2/g_{Cu}) after reaction for 20 h using the summarized results in Table 2. The product values of two characteristics were found to be in the range of 50.1–90.7, and the value was maximized on CZA/Al(2.5)-FER. The results were summarized in Fig. 7 by reconsidering the results of previous work [10]. The results showed a good correlation for structure insensitive characters of a single-step reaction of DME from syngas above the value of 20, which is a product value of acidic sites and surface area of metallic copper. As shown in Fig. 7, TOF values approached a constant value of around 0.07 and reaction rate for around 0.03 above the product value of 20. This observation can be attributed to the fast dehydration rate of methanol DME compared with that of methanol formation by CO hydrogenation on the bifunctional CZA/Al-FER catalysts. Since the rate determining step is known to be methanol synthesis reaction on metallic copper surfaces, and the concomitant dehydration of methanol to DME can be efficiently carried out on weak acidic

Table 3
Catalytic performances of the bifunctional CZA/Al-FER catalysts.^a

| Notation | CO conversion (mol%) | CO conversion to CO ₂ (mol%) | Selectivity of methanol/DME/byproducts ^b (mol%) | Yield of DME (mol%) | Reaction rate ^c /10 ⁻² | TOF ^c /10 ⁻² |
|-----------------|----------------------|---|--|---------------------|--|------------------------------------|
| CZA/Al(0)-FER | 46.6 | 9.4 | 5.1/87.4/7.5 | 32.5 | 2.77 | 5.88 |
| CZA/Al(2.5)-FER | 61.8 | 13.5 | 4.7/93.4/1.9 | 45.2 | 3.68 | 6.07 |
| CZA/Al(5)-FER | 62.1 | 14.5 | 5.7/91.5/2.8 | 43.6 | 3.70 | 6.03 |
| CZA/Al(10)-FER | 43.0 | 7.8 | /91.6/3.5 | 32.2 | 2.56 | 6.86 |

^a Catalytic reaction was conducted under the following conditions for 20 h; $T=250\text{ }^{\circ}\text{C}$, $P=3.5\text{ MPa}$, $SV=2000\text{ ml/g}_{\text{cat}}/\text{h}$, feed composition of $\text{CO}/\text{H}_2/\text{N}_2=31.6/63.2/5.2$. The CO conversion and product distribution are the averaged values after 15 h at steady-state.

^b Byproducts mainly are composed of CH_4 and C_2^+ hydrocarbons.

^c Reaction rate was defined as the reacted CO mol/g_{cat}/h and turn over frequency (TOF) is calculated by using the values of copper surface area after reaction with the equation of the number of reacted CO molecules/surface metallic copper atom/second.

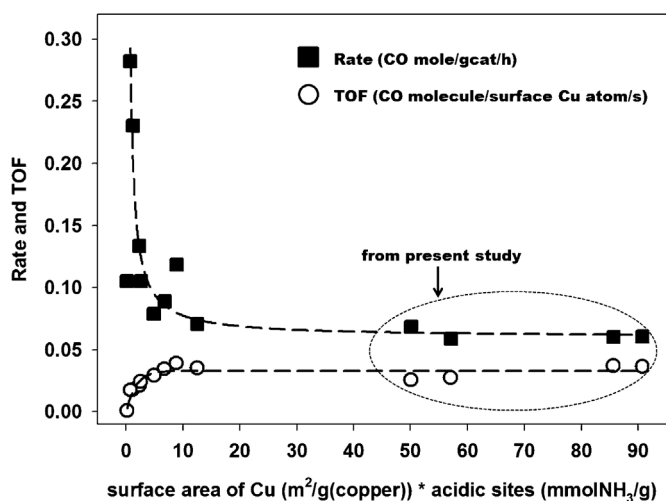


Fig. 7. Reaction rate and intrinsic activity (TOF) of CZA/Al-FER catalysts with respect to the product values of the amount of acidic sites (mmolNH₃/g_{cat}) and surface area of metallic copper (m²/g_{Cu}) after reaction for 20 h (included with the results of Ref. [10]).

sites, the optimum concentration of acidic sites and copper surface area is simultaneously responsible for obtaining a higher catalytic performance which can be controlled by the particle size of copper and the acidic sites on Al₂O₃-modified H-ferrierite surface.

4. Conclusions

Single step synthesis of DME from syngas on the bifunctional CZA/Al-FER catalysts was investigated to elucidate effects of acidic sites and copper surface area to the intrinsic activity. The Al₂O₃ modification of H-ferrierite was found to enhance CO conversion and DME yield by adjusting acidic sites and dispersion of copper particles. The optimum concentration of solid-acid Al₂O₃ modifier was found to be around 2.5–5 wt% on H-ferrierite, and it altered the dispersion of Cu–ZnO–Al₂O₃ particles on H-ferrierite with an enhanced interaction of copper particles and small copper particle formation. It also significantly suppressed the aggregation of copper particles on CZA/Al-FER catalysts with a higher stability. In addition, Al₂O₃ modifier of H-ferrierite is also to reduce strong acidic sites by depositing on the sites selectively and it reduced the byproduct formation. Both of copper surface area and amount of acidic sites are well correlated with an intrinsic activity, which finally shows a structure-insensitive character for a single-step synthesis of DME from syngas. Finally, TOF values approached a constant value of around 0.07 and reaction rate for around 0.03 in terms of the product values of acidic sites and surface area of metallic copper above 20. This intrinsic character can also be attributed to the fast dehydration rate of methanol to DME compared with that of methanol formation by CO hydrogenation on the

bifunctional CZA/Al-FER catalysts. The optimum concentration of acidic sites and copper surface area is responsible for a higher catalytic performance which can be obtained by controlling the particle size of copper on the acidic site by adjusting Al₂O₃-modified H-ferrierite surface on CZA/Al-FER catalysts.

Acknowledgements

The authors would like to acknowledge the financial support from the National Research Foundation of Korea (NRF) grant funded by the Korea government (MEST; 2011-0009003 and 2012R1A2A2A02013876).

Appendix A. Supplementary data

Supplementary data associated with this article can be found, in the online version, at <http://dx.doi.org/10.1016/j.cattod.2013.11.015>.

References

- [1] M. Ruggiero, G. Manfredi, *Renew. Energ.* 16 (1999) 1106–1109.
- [2] N. Armaroli, V. Balzani, *ChemSusChem* 4 (2011) 21–36.
- [3] K.L. Ng, D. Chardwick, B.A. Toseland, *Chem. Eng. Sci.* 54 (1999) 3587–3592.
- [4] D. Song, W. Cho, D.K. Park, E.S. Yoon, *J. Ind. Eng. Chem.* 13 (2007) 815–826.
- [5] J.L. Li, X.G. Zhang, T. Inui, *Appl. Catal. A: Gen.* 147 (1996) 23–33.
- [6] J.H. Fei, M.X. Yang, Z.Y. Hou, X.M. Zheng, *Energy Fuels* 18 (2004) 1584–1587.
- [7] J. Xia, D. Mao, B. Zhang, Q. Chen, Y. Tang, *Catal. Lett.* 98 (2004) 235–240.
- [8] T. Takeguchi, K.I. Yanagisawa, T. Inui, M. Inoue, *Appl. Catal. A: Gen.* 192 (2000) 201–209.
- [9] D. Jim, B. Zhu, Z. Hou, J. Fei, H. Lou, X. Zheng, *Fuel* 86 (2007) 2707–2713.
- [10] J.W. Jung, Y.J. Lee, S.H. Um, P.J. Yoo, D.H. Lee, K.W. Jun, J.W. Bae, *Appl. Catal. B: Environ.* 126 (2012) 1–8.
- [11] J.W. Bae, S.H. Kang, Y.J. Lee, K.W. Jun, *Appl. Catal. B: Environ.* 90 (2009) 426–435.
- [12] S.M. Kim, Y.J. Lee, J.W. Bae, H.S. Potdar, K.W. Jun, *Appl. Catal. A: Gen.* 348 (2008) 113–120.
- [13] S.D. Kim, S.C. Baek, Y.H. Lee, K.W. Jun, M.J. Kim, I.S. Yoo, *Appl. Catal. A: Gen.* 309 (2006) 139–143.
- [14] L. Wang, Y. Qi, Y. Wei, D. Fang, S. Meng, Z. Liu, *Catal. Lett.* 106 (2006) 61–66.
- [15] K. Sun, W. Lu, F. Qiu, S. Liu, X. Xu, *Appl. Catal. A: Gen.* 252 (2003) 243–249.
- [16] D. Mao, W. Yang, J. Xia, B. Zhang, Q. Song, Q. Chen, *J. Catal.* 230 (2005) 140–149.
- [17] J.R. Jensen, T. Johannessen, H. Livbjerg, *Appl. Catal. A: Gen.* 266 (2004) 117–122.
- [18] Konstantin A. Pokrovski, Alexis T. Bell, *J. Catal.* 241 (2006) 276–286.
- [19] J.W. Bae, S.H. Kang, Y.J. Lee, K.W. Jun, *J. Ind. Eng. Chem.* 15 (2009) 566–572.
- [20] P.S. Sai Prasad, J.W. Bae, S.H. Kang, Y.J. Lee, K.W. Jun, *Fuel. Process. Technol.* 89 (2008) 1281–1286.
- [21] E.L. Araceli, J.B. Enrique, S.-P. Regino, S.-S. Antonio, J. Manuel, Martín-Llorente, *Vib. Spectrosc.* 3 (1992) 291–298.
- [22] M. Popova, Á. Szegedi, Z. Cherkezova-Zheleva, A. Dimitrova, I. Mitov, *Appl. Catal. A: Gen.* 381 (2010) 26–35.
- [23] J.W. Bae, H.S. Potdar, S.H. Kang, K.W. Jun, *Energy Fuels* 22 (2008) 223–230.
- [24] Elisabetta Finocchio, Guido Busca, Stefano Rossini, Ugo Cornaro, Valerio Piccoli, Roberta Miglio, *Catal. Today* 33 (1997) 335–352.
- [25] Lijuan Chen, Liping Li, Guangshe Li, *J. Alloys Compounds* 464 (2008) 532–536.
- [26] Z. Zhan, H.C. Zeng, *J. Non-Cryst. Solids* 243 (1999) 26–38.
- [27] S.H. Kang, J.W. Bae, H.S. Kim, G.M. Dhar, J.W. Jun, *Energy Fuels* 24 (2010) 804–810.
- [28] Y. Okamoto, K. Fukino, T. Imanaka, S. Teranishi, *J. Phys. Chem.* 87 (1983) 3740–3747.
- [29] S.R. Blaszkowski, R.A. van Santen, *J. Phys. Chem. B* 101 (1997) 2292–2305.
- [30] B.L. Knier, F. Girgsdies, T. Ressler, *J. Catal.* 236 (2005) 34–44.
- [31] J.H. Flores, M.I.P. da Silva, *Colloid Surf. A* 322 (2008) 113–123.